

3 Fractional Delay Filters

In this chapter we review the digital filter design techniques for the approximation of a *fractional delay* (FD). They can be utilized in many areas of digital signal processing. Examples of these fields are time delay estimation (Smith and Friedlander, 1985), null steering in the direction pattern of antenna arrays (Ko and Lim, 1988), timing adjustment of digital modems (Farrow, 1988; Armstrong and Strickland, 1993; Gardner, 1993; Erup *et al.*, 1993), speech coding (Marques *et al.*, 1989, 1990; Kroon and Atal, 1991; Medan, 1991), speech synthesis (Matsui *et al.*, 1991), and arbitrary sampling-rate conversion (Tarczynski *et al.*, 1994). Fractional delays are essential in digital waveguide models for one-dimensional resonators (Jaffe and Smith, 1983; Laine, 1988; Smith, 1983; Sullivan, 1990; Karjalainen and Laine, 1991; Välimäki *et al.*, 1992a).

There are plenty of design methods for both FIR and IIR fractional delay filters. Only the most useful of them are discussed in detail. A more comprehensive study of known filter design methods for FD approximation has been written by Laakso *et al.* (1994). Of special interest in our applications are digital filters that approximate the ideal interpolation in a maximally flat manner at low frequencies. The maximally flat FIR filter approximation is equivalent to the classical Lagrange interpolation method. This technique is discussed in Section 3.3. The corresponding IIR or allpass filter has a maximally flat group delay response. It is called the Thiran interpolator and is studied in Section 3.4.3. These two design methods appear to be most effective in digital waveguide modeling mainly because they approximate ideal interpolation very accurately at frequencies near the fundamental pitch of speech and music signals.

3.1 Ideal Fractional Delay

We first discuss the concept of fractional delay in continuous and discrete time and consider the ideal solution of the FD problem to show why approximation is necessary.

3.1.1 Continuous-Time System for Arbitrary Delay

Consider a delay element, which is a linear system whose purpose is to delay an incoming continuous-time signal $x_c(t)$ by τ (in seconds). The output signal $y_c(t)$ of this system can be expressed as

$$y_c(t) = x_c(t - \tau) \quad (3.1)$$

where the subscript ‘c’ refers to ‘continuous-time’. The Fourier transform $X_c(\Omega)$ of a continuous-time signal $x_c(t)$ is defined as

$$X_c(\Omega) = \int_{-\infty}^{\infty} x_c(t) e^{-j\Omega t} dt \quad (3.2)$$

where $\Omega = 2\pi f$ is the angular frequency in radians. The Fourier transform $Y_c(\Omega)$ of the delayed signal $y_c(t)$ can be written in terms of $X_c(\Omega)$

$$Y_c(\Omega) = \int_{-\infty}^{\infty} y_c(t) e^{-j\Omega t} dt = \int_{-\infty}^{\infty} x_c(t - \tau) e^{-j\Omega t} dt = e^{-j\Omega\tau} X_c(\Omega) \quad (3.3)$$

The transfer function $H_{\text{id}}(\Omega)$ of the delay element can be expressed by means of Fourier transforms $X_c(\Omega)$ and $Y_c(\Omega)$. This yields

$$H_{\text{id}}(\Omega) = \frac{Y_c(\Omega)}{X_c(\Omega)} = \frac{e^{-j\Omega\tau} X_c(\Omega)}{X_c(\Omega)} = e^{-j\Omega\tau} \quad (3.4)$$

The term $e^{-j\Omega\tau}$ corresponds to the Fourier transform of the delay of τ .

3.1.2 Discrete-Time System for Arbitrary Delay

Next we consider a discrete-time delay system. If the Fourier transform $X_c(\Omega)$ is non-zero only on a finite interval around $\omega = 0$, the continuous-time signal $x_c(t)$ is said to be *bandlimited*. It may then be expressed by its samples $x(nT)$, where $n \in \mathbb{Z}$ is the sample index and T is the sample interval, i.e., the inverse of the sampling rate. For convenience of notation, we omit T and use shortly $x(n)$ to denote the samples of the discrete-time signal.

We want to express the *discrete-time version* of the delay operation for a sampled bandlimited signal. The outgoing discrete-time signal $y(n)$ can simply be written as

$$y(n) = x(n - D) \quad (3.5)$$

where $D = \tau/T$ is the desired delay as multiples of the unit delay. Note that τ/T is generally irrational since τ is usually not an integral multiple of sampling interval T . Unfortunately, Eq. (3.5) is meaningful only for integral values of D . Then the samples of the output sequence $y(n)$ are equal to the delayed samples of the input sequence $x(n)$, and the delay element is called a *digital delay line*. However, if D were real, the delay operation would not be this simple, since the output value would lie somewhere between the known samples of $x(n)$. The sample values of $y(n)$ would then have to be obtained by way of *interpolation* from the sequence $x(n)$.

The spectrum of a discrete-time signal can be expressed by means of the *discrete-time Fourier transform* (DTFT). In this integral transform, the time variable is discretized, but the frequency variable is continuous. The DTFT of signal $x(n)$ is defined as (see, e.g., Roberts and Mullis, 1987, pp. 87–88; Jackson, 1989, pp. 106–118)

$$X(\omega) = \sum_{n=-\infty}^{\infty} x(n) e^{-j\omega n}, \quad |\omega| \leq \pi \quad (3.6)$$

where $\omega = 2\pi fT$ is the normalized angular frequency. The DTFT of the output signal $y(n)$ can be written as

$$Y(\omega) = \sum_{n=-\infty}^{\infty} y(n)e^{-j\omega n} = \sum_{n=-\infty}^{\infty} x(n-D)e^{-j\omega n} = e^{-j\omega D}X(\omega) \quad (3.7)$$

The transfer function of an ideal discrete-time delay element can be given as

$$H_{\text{id}}(\omega) = \frac{Y(\omega)}{X(\omega)} = \frac{e^{-j\omega D}X(\omega)}{X(\omega)} = e^{-j\omega D}, \quad |\omega| \leq \pi \quad (3.8)$$

This is the same result as given in Eq. (3.4)—only now the angular frequency is circular due to discretization in time. In order to be consistent with the z -transform notation used commonly in digital signal processing, let us express the transfer function as

$$H_{\text{id}}(z) = \frac{Y(z)}{X(z)} = \frac{z^{-D}X(z)}{X(z)} = z^{-D} \quad (3.9)$$

where $D \in \mathbb{R}_+$ is the length of the delay in samples. The delay D may be written in the form

$$D = D_{\text{int}} + d \quad (3.10)$$

where $0 \leq d < 1$ is the *fractional delay* and the integer part D_{int} is given by

$$D_{\text{int}} = \lfloor D \rfloor \quad (3.11)$$

where $\lfloor \cdot \rfloor$ is the greatest integer function. It is often called the *floor* function and is defined as

$$\lfloor x \rfloor = \max_{k \leq x} k \quad (3.12)$$

where $x \in \mathbb{R}$ and $k \in \mathbb{Z}$. The block diagram of the ideal delay element is illustrated in Fig. 3.1.

Note that the z -transform representation in (3.9) is used in the Fourier transform sense so that $z = e^{j\omega}$. In principle, the z -transform is defined only for integral powers of z and thus, if D were real, the term z^{-D} should be written as an infinite series making the notation unnecessarily involved.

To understand how to produce a fractional delay using a discrete-time system it is necessary to discuss interpolation techniques. Interpolation of a discrete-time signal is based on the fact that the amplitude of the corresponding continuous-time *bandlimited* signal changes smoothly between the sampling instants.

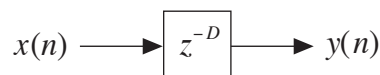


Fig. 3.1 Ideal discrete-time delay element.

3.1.3 Fractional Delay and Shannon Reconstruction

The fractional delay d can in principle have any value between 0 and 1. To be able to produce an arbitrary fractional delay for a discrete-time signal $x(n)$, one has to know a way to compute the amplitude of the underlying continuous-time signal $x(t)$ for all t . This leads us to fundamental issues of digital signal processing—sampling and reconstruction.

In 1949, Shannon introduced the *sampling theorem* (Shannon, 1949). It states that if the Fourier transform $X_c(\Omega)$ of a continuous-time signal $x_c(t)$ is zero outside the interval $(-f_c, f_c)$ then the signal $x_c(t)$ is completely determined by its values at equidistant points spaced $1/2f_c$ apart. This implies that the sampling rate f_s has to be at least $2f_c$. Shannon gave the *reconstruction formula* for a sampled signal using the cardinal series

$$x_c(t) = \sum_{n=-\infty}^{\infty} x(nT) \frac{\sin\left[\frac{\omega_s}{2}(t - nT)\right]}{\frac{\omega_s}{2}(t - nT)} = \sum_{n=-\infty}^{\infty} x(nT) \operatorname{sinc}\left[\frac{\omega_s}{2\pi}(t - nT)\right] \quad (3.13)$$

where $\omega_s = 2\pi f_s$ is the sampling angular frequency in radians per second and T is the corresponding sampling interval, i.e., $T = 1/f_s$. The sinc function is defined as

$$\operatorname{sinc}(t) = \frac{\sin(\pi t)}{\pi t} \quad (3.14)$$

Note that $\operatorname{sinc}(0) = 1$ since $\lim_{t \rightarrow 0} \{\sin(\pi t) / \pi t\} = 1$.

According to Eq. (3.13) the *ideal bandlimited interpolator* has a continuous-time impulse response

$$h_c(t) = \frac{\sin\left(\frac{\omega_s t}{2}\right)}{\frac{\omega_s t}{2}} = \operatorname{sinc}\left(\frac{\omega_s t}{2\pi}\right) \quad (3.15)$$

for $t \in \mathbb{R}$. This impulse response that Shannon called the Whittaker cardinal function converts a discrete-time signal to a continuous-time one. In delay applications, however, it is necessary to know the value of a signal at a single time instant between the samples. The desired result may be obtained by shifting Eq. (3.15) by D and then sampling it at equidistant points. Hence, the output $y(n)$ of the ideal discrete-time fractional delay element is computed as

$$y(n) = x(n - D) = \sum_{k=-\infty}^{\infty} x(k) \operatorname{sinc}(n - D - k) \quad (3.16)$$

for $n \in \mathbb{Z}$ and $D \in \mathbb{R}$. Here we have simplified the notation setting the sampling rate f_s to 1 (and consequently, the sampling interval $T = 1$), since with a discrete-time system description it is not necessary to fix the actual sampling rate.

It can be concluded that producing a fractional delay requires reconstruction of the discrete-time signal and shifted resampling of the resulting continuous-time signal. In Eq. (3.16) these two operations have been combined.

3.1.4 Characteristics of the Ideal Fractional Delay Element

In digital signal processing, it is often advantageous to study linear filters in the frequency domain, that is, by their frequency response. The ideal bandlimited interpolator given by (3.16) has the frequency response obtained from (3.8) as

$$H_{\text{id}}(e^{j\omega}) = e^{-j\omega D}, \quad |\omega| \leq \pi \quad (3.17)$$

The frequency response of the ideal delay element has the following magnitude and phase characteristics

$$|H_{\text{id}}(e^{j\omega})| = 1 \quad (3.18a)$$

$$\arg\{H_{\text{id}}(e^{j\omega})\} = \Theta_{\text{id}}(\omega) = -D\omega \quad (3.18b)$$

In other words, the delay element is a *linear-phase allpass* system. Its *phase delay* and the *group delay* are, respectively,

$$\tau_{\text{p, id}}(\omega) = -\frac{\Theta_{\text{id}}(\omega)}{\omega} = D \quad (3.19a)$$

and

$$\tau_{\text{g, id}}(\omega) = -\frac{\partial\Theta_{\text{id}}(\omega)}{\partial\omega} = D \quad (3.19b)$$

where $\Theta_{\text{id}}(\omega)$ is the ideal phase response as defined in Eq. (3.18b). From these results it can be concluded that the ideal delay element passes all the frequency components of an incoming signal with the same delay D .

The inverse discrete-time Fourier transform of Eq. (3.17) gives the impulse response (IR) of an ideal delay element [compare with Eq. (3.16)] as

$$\begin{aligned} h_{\text{id}}(n) &= \frac{1}{2\pi} \int_{-\pi}^{\pi} H_{\text{id}}(e^{j\omega}) e^{j\omega n} d\omega = \frac{1}{2\pi} \int_{-\pi}^{\pi} e^{-j\omega D} e^{j\omega n} d\omega = \frac{1}{2\pi} \int_{-\pi}^{\pi} e^{j\omega(n-D)} d\omega \\ &= \frac{e^{j\pi(n-D)} - e^{-j\pi(n-D)}}{j2\pi(n-D)} = \frac{\sin[\pi(n-D)]}{\pi(n-D)} = \text{sinc}(n-D) \end{aligned} \quad (3.20)$$

If D is an integer ($d = 0$), the IR of the delay element is zero at all sampling points except at $n = D$, that is

$$d = 0 \Rightarrow h_{\text{id}}(n) = \begin{cases} 1 & \text{for } n = D \\ 0 & \text{otherwise} \end{cases} \quad (3.21)$$

In this case, the delay element is implemented by a cascade of unit delays as discussed earlier. When D is a fractional number, i.e., $0 < d < 1$, the IR has non-zero values at all index values $n \in \mathbb{Z}$, or

$$0 < d < 1 \Rightarrow h_{\text{id}}(n) \neq 0 \quad \text{for all } n \quad (3.22)$$

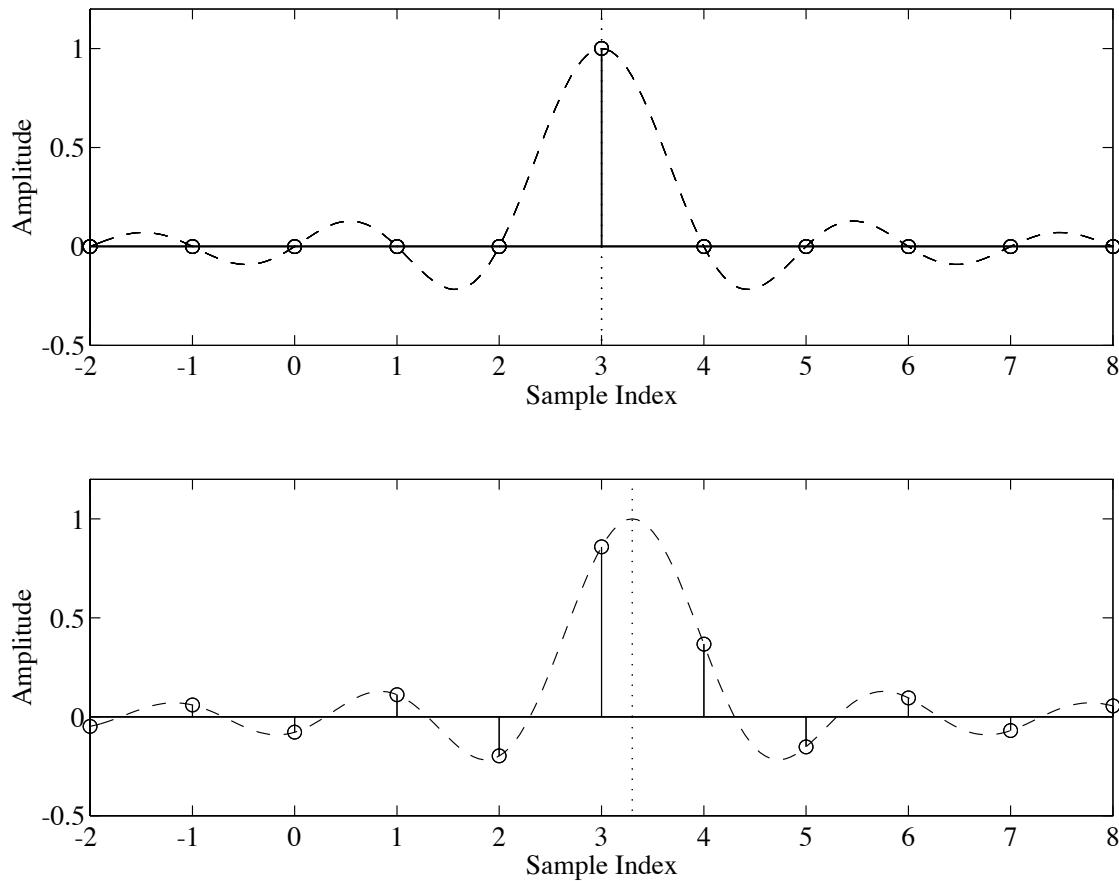


Fig. 3.2 (Upper) The sinc function (dashed line) shifted by $D = 3.0$. The circles indicate the sampled values of the sinc function. All the sample values except the centermost are zero when the delay is an integer, that is $d = 0$. (Lower) The sinc function shifted by $D = 3.3$. The dotted line indicates the center point of the shifted sinc function. This figure illustrates the fact that all the sample values (circles) are non-zero in the case of a fractional delay, i.e., $d \neq 0$.

These time-domain properties of the ideal delay element are illustrated in Fig. 3.2. In the upper part of this figure, the delay D is an integer and only one sample is non-zero because the zero crossings of the sinc function coincide with the other sampling points. In the lower part of Fig. 3.2, however, the delay D is a fractional number and all the samples on the interval $(-\infty, \infty)$ are non-zero.

To conclude, the impulse response $h_{\text{id}}(n)$ of the delay element is a shifted and sampled version of the sinc function which is infinitely long. Due to this the IR corresponds to a *noncausal* filter which cannot be made causal by a finite shift in time. In addition, the filter is not BIBO[†] stable since the impulse response (3.20) is not absolutely summable. This kind of filter is *nonrealizable*. To produce a realizable fractional delay filter, some finite-length approximation for the sinc function has to be used.

Before considering these approximations we notify one particular property of the ideal transfer function that makes the fractional delay approximation difficult. The imaginary part of the ideal transfer function is

[†] BIBO is short for Bounded Input Bounded Output.

$$\operatorname{Im}\left\{H_{\text{id}}(e^{j\omega})\right\}\Big|_{\omega=\pi} = -\sin(\pi D) \quad (3.23)$$

This implies that when D is a fractional number, the transfer function has a complex value at $\omega = \pi$. Discrete-time filters with real coefficients have the property that

$$H(e^{j\omega})\Big|_{\omega=\pi} \in \mathbb{R} \quad (3.24)$$

This implies that, at the Nyquist frequency, the approximation error cannot be smaller than $|\sin(\pi D)|$. Cain and Yardim (1994) call this the *Tarczynski bound*.

Some of the useful fractional delay approximation techniques will be discussed in the following sections.

3.1.5 Conclusion and Discussion

Up to now we have discussed the theoretical background of noninteger digital delay, or fractional delay. The relationship between the underlying analog signal and fractional delay was clarified. Furthermore, the characteristics of the ideal fractional delay element were reviewed and it was shown that the ideal FD system (i.e., ideal bandlimited interpolator) is nonrealizable, since the corresponding impulse response is infinitely long and noncausal. Thus, approximation techniques have to be employed to obtain a finite-length causal implementation of FD.

Formerly, similar theoretical aspects have been considered in the context of signal recovery and multirate signal processing. Implementation of a fractional delay requires that the system is in principle able to compute the amplitude of the signal at any time instant between known samples. Thus, the FD problem and recovery of an analog signal from its samples are essentially equivalent.

The major differences between the FD problem and sampling-rate conversion are as follows.

- 1) In FD processing only one new sample per sampling interval needs to be computed, whereas in interpolation for increasing the sampling rate, several new samples per original sample interval may be needed.
- 2) In the FD problem the fractional interval d to be approximated is in general irrational, whereas in sample-rate conversions, simple rational ratios are often used.

The underlying theory of these two DSP problems is, of course, the same.

Even today, FD processing is not a well-known topic in signal processing. Discussion on this topic has appeared only in few textbooks (see, e.g., Crochiere and Rabiner, 1983, pp. 271–274; Regalia, 1993, pp. 948–953).

3.2 Design Methods for Fractional Delay FIR Filters

In this section, the FIR filter approximation of the fractional delay is discussed. For more detailed discussion and examples see Laakso *et al.* (1994). A comparison of four FD FIR filter design methods has been made by Cain *et al.* (1994).

The transfer function of an FIR filter is of the form

$$H(z) = \sum_{n=0}^N h(n)z^{-n} \quad (3.25)$$

where N is the order of the filter and $h(n)$ ($n = 0, 1, \dots, N$) are the real coefficients that form the impulse response of the FIR filter. Note that the length of the impulse response (i.e., the number of the filter coefficients) is

$$L = N + 1 \quad (3.26)$$

In the design procedure our aim is to minimize the *error function* defined by

$$E(e^{j\omega}) = H(e^{j\omega}) - H_{\text{id}}(e^{j\omega}) \quad (3.27)$$

i.e., the difference of the ideal frequency response and the approximation.

3.2.1 Least Squared Integral Error Design

The intuitively most attractive method for designing realizable FD filters is certainly the truncation of the ideal IR defined by Eq. (3.20). This method minimizes the least squared (LS) error function E_{LS} which is equal to the L_2 norm (integrated squared magnitude) of the error frequency response $E(e^{j\omega})$, that is

$$E_{\text{LS}} = \frac{1}{\pi} \int_0^{\pi} |E(e^{j\omega})|^2 d\omega = \frac{1}{\pi} \int_0^{\pi} |H(e^{j\omega}) - H_{\text{id}}(e^{j\omega})|^2 d\omega \quad (3.28)$$

Using Parseval's relation this equation can be converted into the time domain. This results in

$$E_{\text{LS}} = \sum_{n=-\infty}^{\infty} |h(n) - h_{\text{id}}(n)|^2 = \sum_{n=-\infty}^{\infty} [h_{\text{id}}^2(n) + h^2(n) - 2h(n)h_{\text{id}}(n)] \quad (3.29)$$

From this equation, it is possible to derive a closed-form solution for the squared integral error in the case of fractional delay approximation. According to Parseval's relation, the first term in (3.29) can be evaluated in the following way:

$$\sum_{n=-\infty}^{\infty} |h_{\text{id}}(n)|^2 = \frac{1}{\pi} \int_0^{\pi} |H_{\text{id}}(e^{j\omega})|^2 d\omega = \frac{1}{\pi} \int_0^{\pi} |e^{-j\omega D}|^2 d\omega = 1 \quad (3.30)$$

The second and third term of Eq. (3.29) include the coefficients of the N th-order FIR filter and thus the summation indices can be limited. The closed-form solution is

$$E_{\text{LS}} = 1 + \sum_{n=0}^N [h^2(n) - 2h(n)\text{sinc}(n - D)] \quad (3.31)$$

where the sinc function is defined by Eq. (3.14).

It is also possible to derive a closed-form formula for the bandlimited squared integral error. The derivation is presented in Appendix A.

According to Eq. (3.31), the optimal solution for an N th-order FIR filter in the L_2 sense is obviously the one with $N + 1$ coefficients truncated symmetrically around the

maximum value, i.e., the central point of $h_{\text{id}}(n)$. The approximation error resulting from this approach may be written as

$$E_{\text{LS}} = \sum_{n=-\infty}^{-1} |h_{\text{id}}(n)|^2 + \sum_{n=N+1}^{\infty} |h_{\text{id}}(n)|^2 \quad (3.32)$$

It is seen that the approximation error decreases as N increases. This is intuitively clear. The impulse response $h(n)$ of the LS FD FIR filter can be expressed as

$$h(n) = \begin{cases} \text{sinc}(n - D), & 0 \leq n \leq N \\ 0, & \text{otherwise} \end{cases} \quad (3.33)$$

The delay D should be located between the two central taps of the filter when N is odd ($L = N + 1$ is even), or within half a sample from the central tap when N is even (L odd), since then the approximation error is smallest. This means that the delay D should be chosen so that the following inequality is valid:

$$\frac{N-1}{2} \leq D \leq \frac{N+1}{2} \quad (3.34)$$

For odd-order FIR interpolators (N odd and L even) this simply implies that the integer part D_{int} of the delay has to be chosen in the following way:

$$D_{\text{int}} = \frac{N-1}{2} \quad (3.35)$$

When N is even (L odd) the integer part of the delay should be chosen so that

$$D_{\text{int}} = \begin{cases} \frac{N}{2} & \text{when } 0 \leq d < \frac{1}{2} \\ \frac{N}{2} - 1 & \text{when } \frac{1}{2} \leq d < 1 \end{cases} \quad (3.36)$$

This will ensure that point D is located within half a sample from the midpoint of the interpolator and consequently that the approximation error is smallest possible with the used FIR design technique.

Above we have assumed that the FIR filter coefficients are truncated from the beginning of the ideal impulse response. This is not the only possible choice. The index M of the first non-zero sample should be chosen in the following way:

$$M = \begin{cases} \text{round}(D) - \frac{N}{2} & \text{for even } N \\ \lfloor D \rfloor - \frac{N-1}{2} & \text{for odd } N \end{cases} \quad (3.37)$$

where $\text{round}(\cdot)$ denotes the operation of rounding to the nearest integer, and $\lfloor \cdot \rfloor$ is the greatest integer function as given by Eq. (3.12). The FIR filter $h(n)$ will be *causal* if $M \geq 0$. If $M < 0$, the filter will be *noncausal* and thus *nonrealizable*. An integer must then be added to D in order to shift the central point of the sinc function so that the requirement of Eq. (3.34) is fulfilled. This is equivalent to adding unit delays to the delay line.

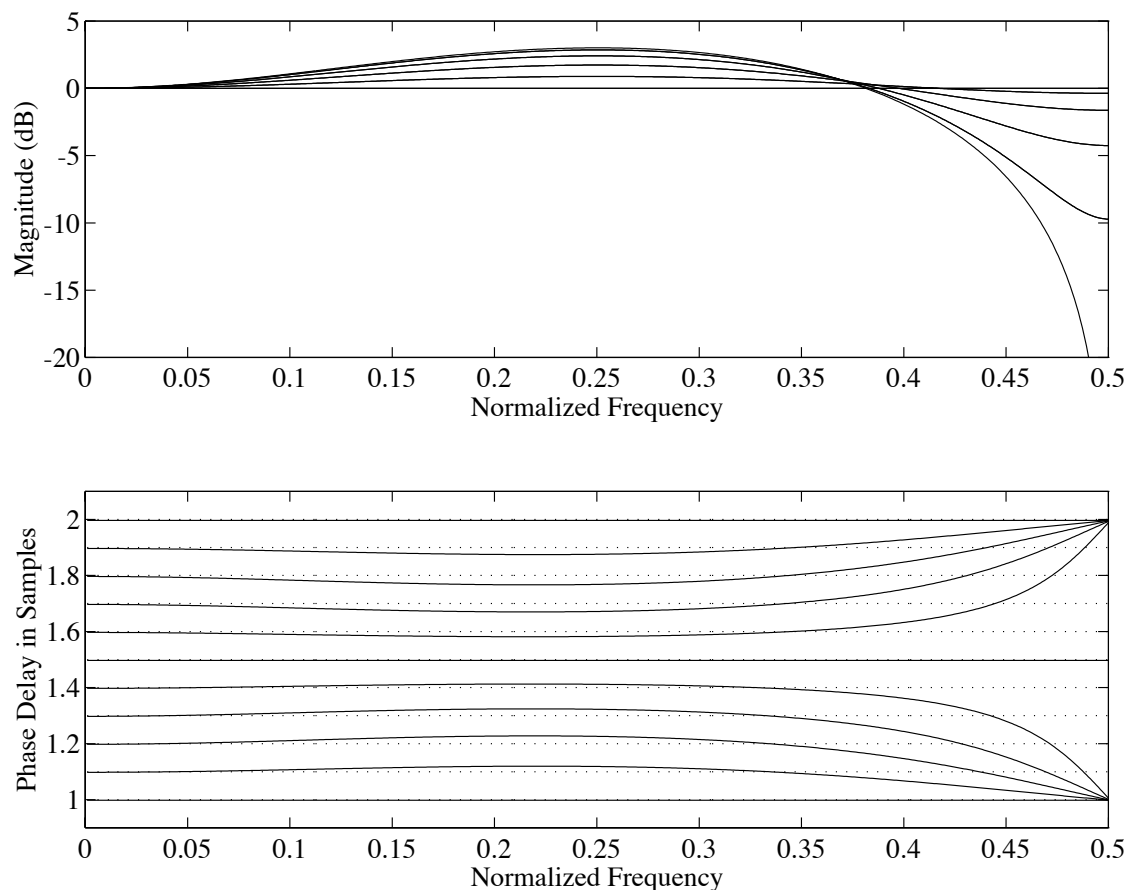


Fig. 3.3 Magnitude responses (upper) and phase delay curves (lower) of a third-order FIR filter designed by truncating the shifted sinc function. The curves are plotted for 11 fractional delay values between 1.0 and 2.0. Note that the magnitude responses for $N - D$ are the same as for D .

However, unit delays cannot be added if the actual delay D , including the integer part, is important. Another method to make the FIR filter causal is to choose a smaller value for N , that is, to design a filter of lower order. This will obviously make the approximation less accurate.

If Eq. (3.31) is valid, then $M = 0$ and the entire delay D is implemented by the FIR filter. This case corresponds to the best (highest-order) causal approximation but also to the heaviest computational load that an LS FIR filter can offer. If $M > 0$ then part of the desired delay has to be implemented by a sequence of unit delays while the rest of that delay is approximated by the FD filter. The implementation of a fractional delay with FIR filters will be discussed further in Sections 3.5.2 and 4.1.

Truncating the shifted sinc function is an easy way to design FD FIR filters. This approach has been proposed, e.g., by Sivanand *et al.* (1991) (see also Sivanand, 1992) and Cain *et al.* (1994). However, it is often not useful since truncation of the impulse response introduces ripple to the frequency response. This is called the *Gibbs phenomenon*. It causes the maximum deviation from the ideal frequency response to remain approximately constant irrespective of the filter order. This goes for both the magnitude and the phase response.

The magnitude and phase delay characteristics of an LS FD FIR filter are illustrated in Fig. 3.3. The order N of the filter is 3 and thus the best approximation ($M = 0$) is

obtained with delay values $1 \leq D < 2$. Were $N = 4$, M would be 0 for $1.5 \leq D < 2.5$. Notice the overshoot in both the magnitude and the phase delay curves. It is seen that the phase delay curves are symmetrical with respect to the delay of 1.5 samples, which corresponds to the central point of the filter's impulse response.

3.2.2 LS Design with Reduced Bandwidth

A variation of the LS design technique is to use a *lowpass* interpolator as a prototype filter instead of a fullband filter (Laakso *et al.*, 1994). The ideal solution is then defined in the interval $[0, \alpha\pi]$ where $0 < \alpha < 1$. The solution corresponding to Eq. (3.33) is now

$$h(n) = \begin{cases} \frac{\sin[\alpha\pi(n-D)]}{\pi(n-D)} & \text{for } M \leq n \leq M+N \\ 0 & \text{otherwise} \end{cases} \quad (3.38)$$

with M defined as in Eq. (3.37). It appears that the Gibbs phenomenon will be reduced considerably, as desired, but the usable bandwidth will contract by α . Thus we conclude that narrowing the bandwidth does not necessarily improve the LS FD filter design.

Another variation of the basic LS design is to use a reduced bandwidth with a *smooth transition band* function (Parks and Burrus, 1987, pp. 63–70). This will make the impulse response of the FD element decay fast. The IR will still be infinitely long and must be truncated, but the Gibbs phenomenon is guaranteed to be reduced, since the discontinuity is not as sharp as originally. A good choice for the transition band is a low-order spline multiplied by $e^{-j\omega D}$. Using this design the magnitude response of the FD FIR filter will remain constant with high precision. However, the price paid is that the phase response will be severely nonlinear (Laakso *et al.*, 1994).

3.2.3 Windowing the Ideal Impulse Response

A well-known method to reduce the Gibbs phenomenon in FIR filter design is to use a bell-shaped window function for weighting in the time domain (see, e.g., Parks and Burrus, 1987, pp. 71–83). Truncation corresponds to windowing with a rectangular window function. An extensive tutorial on window functions and their properties has been written by Harris (1978). The impulse response of an FIR filter designed by the windowed LS method can be written in the form

$$h(n) = \begin{cases} w(n-D)\text{sinc}(n-D) & \text{for } M \leq n \leq M+N \\ 0 & \text{otherwise} \end{cases} \quad (3.39)$$

Note that the midpoint of the window function $w(n)$ of length $N+1$ has been shifted by D so that the shifted sinc function will be windowed symmetrically with respect to its center. The window function $w(n-D)$ is *asymmetric*, however. Many window functions, such as the Hamming and von Hann windows, can be easily delayed by a fractional value D (Laakso *et al.*, 1994; Cain and Yardim, 1994; Cain *et al.*, 1994, 1995) whereas some others cannot. For instance, there is no known method to design exact fractionally shifted Dolph–Chebyshev or Saramäki windows for an arbitrary D . This is because these windows have been designed in the frequency domain. An approximative technique for shifting these windows has been proposed by Laakso *et al.* (1995b).

It is readily seen that the approximation error E_{LS} [see Eq. (3.29)] will be larger with

a window function than without it [see Eq. (3.32)]. Thus, this design method does not minimize the LS error measure, but it is an *ad hoc* modification of the LS technique. In general, the frequency response of an FD FIR filter designed using this technique has a lower ripple but also a wider transition band than a corresponding LS filter (see, e.g., Parks and Burrus, 1987, p. 73). A drawback is that the control of the magnitude error is difficult when changing the parameters of, e.g., the Kaiser or the Dolph–Chebyshev window.

The windowing method is suitable for real-time systems where the fractional delay is changed since the coefficients can be updated quickly. The samples of the sinc and the window function can be stored in memory for several values of D . The filter coefficients for delay values between the stored ones may be obtained, e.g., by linear interpolation (Smith and Gossett, 1984). Smith (1992a) has studied the implementation and error analysis of this kind of interpolator in detail.

3.2.4 General Least Squares FIR Approximation of a Complex Frequency Response

In principle, the FIR fractional delay filter with the smallest LS error in the defined approximation band is accomplished by defining the response only in that part of the frequency band and by leaving the rest out of the error measure as a ‘don’t care’ band (Laakso *et al.*, 1994). This scheme also enables frequency-domain weighting of the LS error. This technique is called general least squares (GLS) FIR filter approximation, and it results in the following error function

$$E_{\text{GLS}} = \frac{1}{\pi} \int_0^{\alpha\pi} W(\omega) |E(e^{j\omega})|^2 d\omega = \frac{1}{\pi} \int_0^{\alpha\pi} W(\omega) |H(e^{j\omega}) - H_{\text{id}}(e^{j\omega})|^2 d\omega \quad (3.40)$$

where the error is defined in the lowpass frequency band $[0, \alpha\pi]$ only and $W(\omega)$ is the nonnegative frequency-domain weighting function [which has nothing to do with the time-domain window function $w(n)$]. The derivation of the bandlimited squared integral error function for the case $W(\omega) \equiv 1$ is presented in Appendix A. Now it is shown how a filter design algorithm can be obtained based on this approach.

The DTFT of the FIR filter can be written as

$$H(e^{j\omega}) = \mathbf{h}^T \mathbf{e} \quad (3.41a)$$

where \mathbf{h} is the coefficient vector

$$\mathbf{h} = [h(0) \quad h(1) \quad \dots \quad h(N)]^T \quad (3.41b)$$

and \mathbf{e} is defined as

$$\mathbf{e} = [1 \quad e^{-j\omega} \quad \dots \quad e^{-jN\omega}]^T \quad (3.41c)$$

The error function (3.40) can now be rewritten in the following way:

$$E_{\text{GLS}} = \frac{1}{\pi} \int_0^{\alpha\pi} W(\omega) [\mathbf{h}^T \mathbf{e} - H_{\text{id}}(e^{j\omega})] [\mathbf{h}^T \mathbf{e} - H_{\text{id}}(e^{j\omega})]^* d\omega \quad (3.42)$$

where the superscript ‘*’ denotes complex conjugation. This equation can be further elaborated as

$$E_{\text{GLS}} = \frac{1}{\pi} \int_0^{\alpha\pi} W(\omega) \left[\mathbf{h}^T \mathbf{C} \mathbf{h} - 2\mathbf{h}^T \operatorname{Re}\{H_{\text{id}}(e^{j\omega}) \mathbf{e}^*\} + |H_{\text{id}}(e^{j\omega})|^2 \right] d\omega \quad (3.43a)$$

where

$$\mathbf{C} = \operatorname{Re}\{\mathbf{e}\mathbf{e}^H\} = \begin{bmatrix} 1 & \cos(\omega) & \cdots & \cos(N\omega) \\ \cos(\omega) & 1 & & \cos[(N-1)\omega] \\ \vdots & & \ddots & \vdots \\ \cos(N\omega) & \cos[(N-1)\omega] & \cdots & 1 \end{bmatrix} \quad (3.43b)$$

Here the superscript ‘ H ’ stands for the Hermitian operation, i.e., transposition with conjugation. The error function can further be expressed as

$$E_{\text{GLS}} = \mathbf{h}^T \mathbf{P} \mathbf{h} - 2\mathbf{h}^T \mathbf{p}_1 + p_0 \quad (3.44a)$$

where we have used the following matrices and vectors:

$$\mathbf{P} = \frac{1}{\pi} \int_0^{\alpha\pi} W(\omega) \mathbf{C} d\omega \quad (3.44b)$$

$$\mathbf{p}_1 = \frac{1}{\pi} \int_0^{\alpha\pi} W(\omega) \left[\operatorname{Re}\{H_{\text{id}}(e^{j\omega})\} \mathbf{c} - \operatorname{Im}\{H_{\text{id}}(e^{j\omega})\} \mathbf{s} \right] d\omega \quad (3.44c)$$

$$p_0 = \frac{1}{\pi} \int_0^{\alpha\pi} W(\omega) |H_{\text{id}}(e^{j\omega})|^2 d\omega \quad (3.44d)$$

$$\mathbf{c} = [1 \quad \cos(\omega) \quad \cdots \quad \cos(N\omega)]^T \quad (3.44e)$$

and

$$\mathbf{s} = [0 \quad \sin(\omega) \quad \cdots \quad \sin(N\omega)]^T \quad (3.44f)$$

The optimal solution in terms of the L_2 norm is obtained by solving for the minimum of the error measure (3.44a). The unique minimum-error solution is found by setting its derivative with respect to \mathbf{h} to zero. This results in the following *normal equation*

$$2\mathbf{P}\mathbf{h} - 2\mathbf{p}_1 = 0 \quad (3.45)$$

which is solved formally by matrix inversion, i.e.,

$$\mathbf{h} = \mathbf{P}^{-1} \mathbf{p}_1 \quad (3.46)$$

In practice, the optimal solution is obtained by determining the integrals involved in Eqs. (3.44) (usually numerically) and solving the set of $N + 1$ linear equations (3.46). Numerical problems may arise, particularly in narrowband approximation (Laakso *et al.*, 1994). However, in FD filter design this is not typical. The design is much easier if

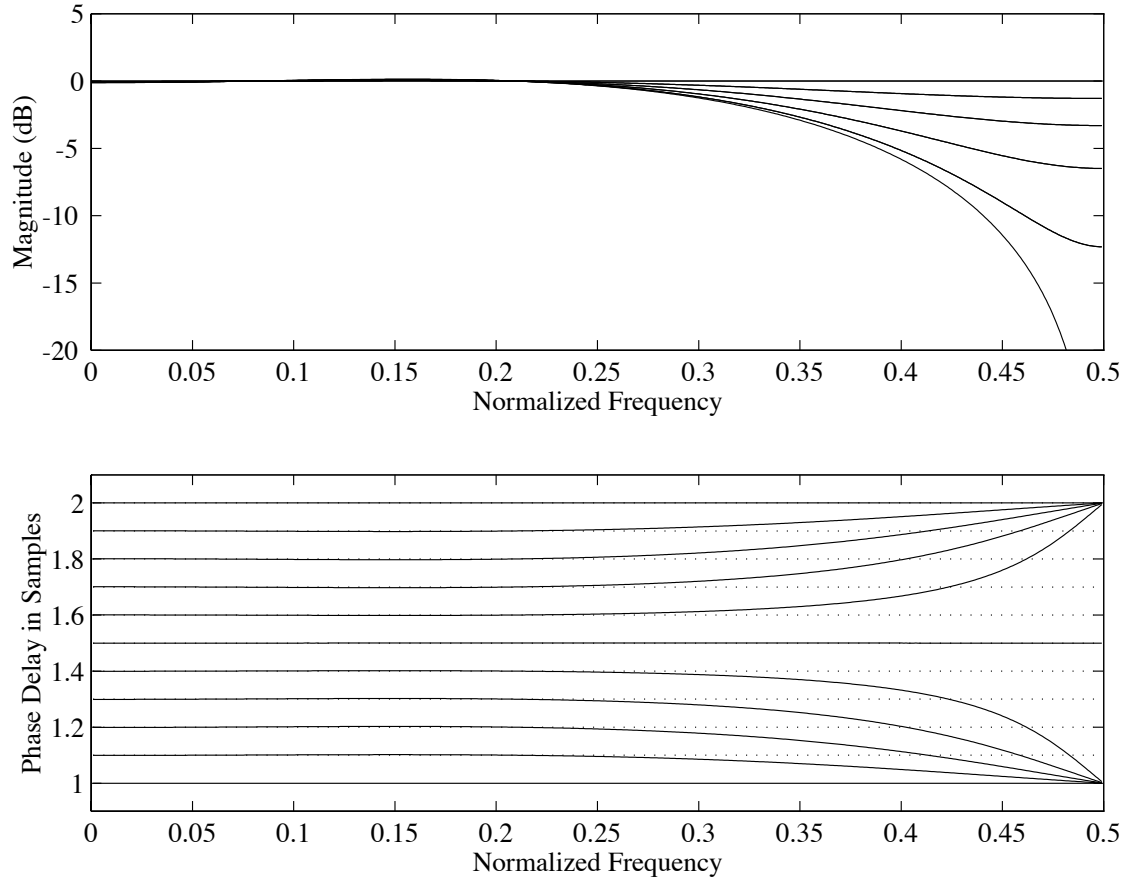


Fig. 3.4 Magnitude responses (upper) and phase delay curves (lower) of a third-order GLS FIR filter with $\alpha = 0.5$. The curves are plotted for 11 fractional delay values between 1.0 and 2.0. Note that the magnitude responses for $N - D$ are the same as for D .

the weighting function is not used, i.e., $W(\omega) \equiv 1$, since the solution can be given in closed form. Then elements of \mathbf{P} and \mathbf{p}_1 can be expressed as

$$P_{k,l} = \frac{1}{\pi} \int_0^{\alpha\pi} \cos[(k-l)\omega] d\omega = \alpha \text{sinc}[\alpha(k-l)] \quad k, l = 1, 2, \dots, L \quad (3.47)$$

and

$$p_{1,k} = \frac{1}{\pi} \int_0^{\alpha\pi} \cos[(k-D)\omega] d\omega = \alpha \text{sinc}[\alpha(k-D)] \quad k = 1, 2, \dots, L \quad (3.48)$$

Note that matrix \mathbf{P} is independent of the delay parameter D and only needs to be inverted once. The resulting FIR filter coefficients depend on the choice of frequency band parameter α and the weighting function.

Figure 3.4 presents a third-order GLS filter with unity weighting function $W(\omega) \equiv 1$ and $\alpha = 0.5$ (i.e., halfband approximation). This result can be compared with the full-band LS FIR approximation of Fig. 3.3. It is seen that the maximum error in both magnitude and phase delay has been reduced in the approximation band. At high frequencies the error has slightly increased since now the approximation error outside the pass-

band $[0, 0.5\pi]$ has not been considered in the design.

3.2.5 Minimax Design of FIR FD Filters

If it is desired to minimize the peak approximation error, it is suitable to use the *minimax* or *Chebyshev* design. These approximation problems can usually be solved only by iterative techniques. Advanced algorithms for complex approximation with minimax error characteristics have been presented, e.g., by Parks and Burrus (1987), Pyfer and Ansari (1987), Preuss (1989), Schulist (1990), Alkhairy *et al.* (1991), and Karam and McClellan (1995). For a more detailed discussion on minimax FIR FD filters, see Laakso *et al.* (1994).

Here we consider a technique proposed by Oetken (1979). The observation that led to the development of this design method is that the magnitude error functions $|E(e^{j\omega})|$ of odd-order equiripple FIR FD filters are almost exactly proportional to each other over the whole frequency range. This implies that it is only needed to determine one optimal filter (the Chebyshev prototype filter), calculate the zeros of its magnitude error function, and then use these zeros to design other FIR FD filters with similar characteristics.

The following discussion has been adapted from Laakso *et al.* (1994). Let us consider that an N th-order (with odd N) symmetric FIR filter has been designed. This filter must approximate flat magnitude response in the equiripple sense in the passband. The error function of this filter has $K = L/2 - 1$ zeros, i.e.

$$E(e^{j\omega}) = H(e^{j\omega}) - H_{\text{id}}(e^{j\omega}) = 0, \quad \omega = \Omega_k, \quad k = 1, 2, \dots, K \quad (3.49)$$

implying that

$$\sum_{n=0}^N h(n)e^{-jn\Omega_k} = e^{-j\Omega_k N/2}, \quad k = 1, 2, \dots, K \quad (3.50)$$

where $N/2$ is the delay of the filter. The filter coefficients can be solved from (3.50) for a chosen total delay D which is close to $N/2$. This can be expressed in matrix form as

$$\mathbf{E}_{\Omega} \mathbf{h} = \mathbf{e}_D \quad (3.51a)$$

where \mathbf{E}_{Ω} is a $K \times (N + 1)$ matrix defined by

$$\mathbf{E}_{\Omega} = \begin{bmatrix} 1 & e^{-j\Omega_1} & e^{-j2\Omega_1} & \dots & e^{-jN\Omega_1} \\ 1 & e^{-j\Omega_2} & e^{-j2\Omega_2} & \dots & e^{-jN\Omega_2} \\ \vdots & \vdots & \vdots & \dots & \vdots \\ 1 & e^{-j\Omega_K} & e^{-j2\Omega_K} & \dots & e^{-jN\Omega_K} \end{bmatrix} \quad (3.51b)$$

and

$$\mathbf{e}_D = \begin{bmatrix} e^{-jD\Omega_1} & e^{-jD\Omega_2} & \dots & e^{-jD\Omega_K} \end{bmatrix}^T \quad (3.51c)$$

Equation (3.51) is a set of K complex equations with $L = 2K$ unknowns, which can be expressed as a fully determined set of L real equations by equating the real and imaginary parts of both sides as

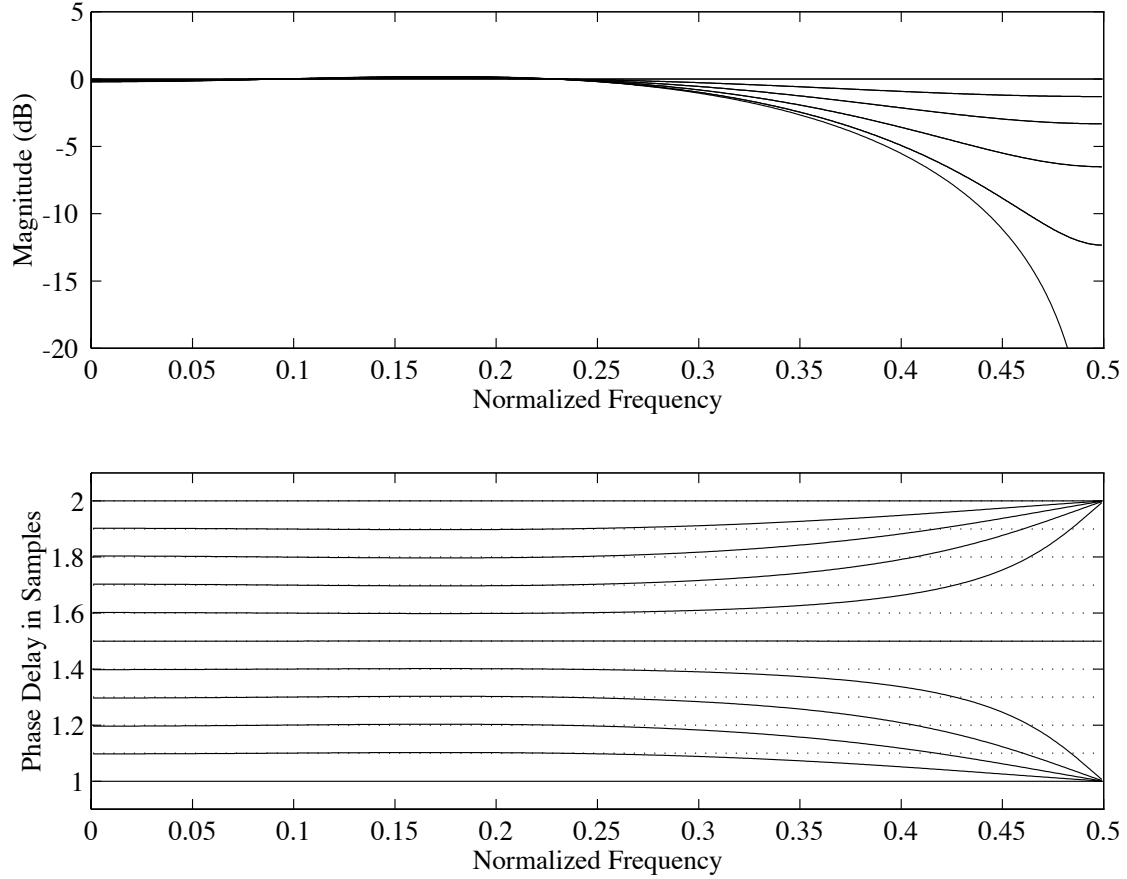


Fig. 3.5 The magnitude and phase delay responses of a third-order ($N = 3$) approximately equiripple FIR FD filter. The curves are plotted for 11 delay values between 1.0 and 2.0. Note that the magnitude responses for $N - D$ are the same as those for D .

$$\mathbf{P}_\Omega \mathbf{h} = \mathbf{p}_\Omega \quad (3.52a)$$

with

$$\mathbf{P}_\Omega = \begin{bmatrix} \mathbf{C}_\Omega \\ \mathbf{S}_\Omega \end{bmatrix} \quad (3.52b)$$

and

$$\mathbf{p}_\Omega = \begin{bmatrix} \mathbf{c}_D \\ \mathbf{s}_D \end{bmatrix} \quad (3.52c)$$

where the matrices and vectors contain appropriate cosine and sine elements such that $\mathbf{E}_\Omega = \mathbf{C}_\Omega - j\mathbf{S}_\Omega$ and $\mathbf{e}_D = \mathbf{c}_D - js_D$. The coefficient vector of the almost-equiripple FIR FD filter is obtained as

$$\mathbf{h} = \mathbf{P}_\Omega^{-1} \mathbf{p}_\Omega \quad (3.53)$$

Note that the cosine-sine matrix \mathbf{P}_Ω depends only on the prototype filter but not on the delay parameter D . Thus it can be inverted once and the same inverse matrix can be

used for approximating FD filters for several values of D .

An example of third-order equiripple FIR FD filters designed using Oetken's method is shown in Fig. 3.5. The prototype filter is a linear-phase halfband ($\alpha = 0.5$) equiripple FIR filter designed using the Remez algorithm (see, e.g., Parks and Burrus, 1987). Figure 3.5 can be compared with Figs. 3.3 and 3.4. It is apparent that at the lower half of the frequency band the equiripple design (Fig. 3.5) yields a much more accurate approximation than the LS approximation (Fig. 3.3). However, the result is comparable to the halfband GLS filter of Fig. 3.4. In both of these figures, the magnitude and phase response curves oscillate around the nominal value at the lower half of the frequency band, and show lowpass behavior at high frequencies.

3.2.6 Other Methods for the Design of FIR FD Filters

In principle, many general FIR filter design techniques may also be applied to the design of FD filters. Altogether, there is a large variety of methods, some of which are mentioned in the following. These techniques are not discussed in detail because they have not appeared to be very useful.

Oetken *et al.* (1975) proposed a *stochastic approach* to the design of interpolating filters. In this technique, the design criterion is the minimum expectable mean squared output error. It appears that this is mathematically equivalent to the general LS design with the frequency-domain weighting function being equal to the average power spectrum of the input signal (Laakso *et al.*, 1994). All the LS methods can also be modified so that the desired frequency response is sampled using a uniform or nonuniform grid.

The maximally flat FD filter design seems to be appropriate for digital waveguide systems since it approximates the ideal bandlimited interpolator very accurately at low frequencies, and its magnitude response never exceeds unity. For these reasons we examine this technique in detail in the following.